Imperial College London

Imperial College London

Department of Aeronautics

Vibration of an aircraft model

Author: Yaroslav Kazakov (CID: 01334502)
Academic responsible: Prof. Silvestre Taviera Pinho
Marker and demonstrator: Mr. Athanasios Giannenas

Date: December 3, 2018

Abstract

This report contains a detailed analysis of the dynamic response of an aircraft model. Students tested the model structure at different applied frequencies and collected magnitude values and phase shift. This allowed students to identify the first mode shape and find the undamped resonant frequency of the aircraft at a specific mass point, which in the experiment was about 17.34 Hz. Understanding the features of a dynamic response of a certain structure helps engineers to predict and avoid a spectrum of structural failures.

Contents

List of Tables

List of Figures

1 Introduction

1.1 Context and Motivation

The experiment allows students to understand the significance of a dynamic response of a particular structure. The behaviour of any real-life (not only a model aircraft) structure can be predicted using the experimental tools and procedures described in the laboratory handout (1). The effects of the dynamic response are crucial since it allows engineers to understand at what frequency will the structure fail or undergo undesirable displacements and stresses. The dynamic structural analysis has an application in the modern world. For instance, test pilots from Airbus performed a flutter (phenomenon that causes structural failure) test on A380 (Figure 1) to acquire the highest possible dive Mach number.

Figure 1: A380 Flutter Test.

All assumptions are listed in Section 4.

1.2 Objectives

The objectives of the experiment are:

1. to measure the first undamped natural frequency of the model aircraft, by:
   (a) using the information contained in the magnitude of the velocity v.s. frequency data
   (b) using the information contained in the phase of the velocity v.s. frequency data
2. to measure the modal damping of the aircraft model for the first type
3. to measure the first modal shape

2 Experimental Procedure

The model aircraft was freely suspended by a wire attached to the fuselage nose and the shakers were connected along the wings and the fuselage at different points (See Figure 13). First of all, all pieces of equipment were switched on in a specific order: computer, conditioning unit and amplifier. It was essential to launch the computer first, to prevent the shakers from receiving noise damage through the amplifier. After the devices were successfully started, Measure Foundry software was opened on the desktop where students could input frequencies and amplification factors. The frequency values were changed by increments in the range from 17.00 Hz to 18.00 Hz. As an output, the software returned acceleration magnitude and phase difference, which are required for the objectives of the experiment. It is worth to mention that the experimental load amplitude factor differed from the one suggested in the handout; (0.055 V) the supervisor recommended this due to a lower chance of signal saturation.

Then the mode shape data was monitored, i.e. amplitude and acceleration magnitude at each concentrated mass. The oscilloscope readings were used to identify in-phase and out-of-phase points on the aircraft. The students then verified that the oscillations of the model followed the theoretically predicted first mode shape.

3 Experimental Results

3.1 Undamped Natural Frequency and Modal Damping Ratio

3.1.1 Experimental Data

A raw data set (3) which is used to plot the graphs below can be found in Appendix B. For one of the frequencies (17.32 Hz) a phase angle could not be read due to significant fluctuations in its value; therefore this data point was ignored in the further analysis.

3.1.2 Frequency Response

All three magnitude curves normalised by the load factor against the forcing frequency are plotted (see Figure 2). The separate sketches are plotted as well (Figure 3 to 5).

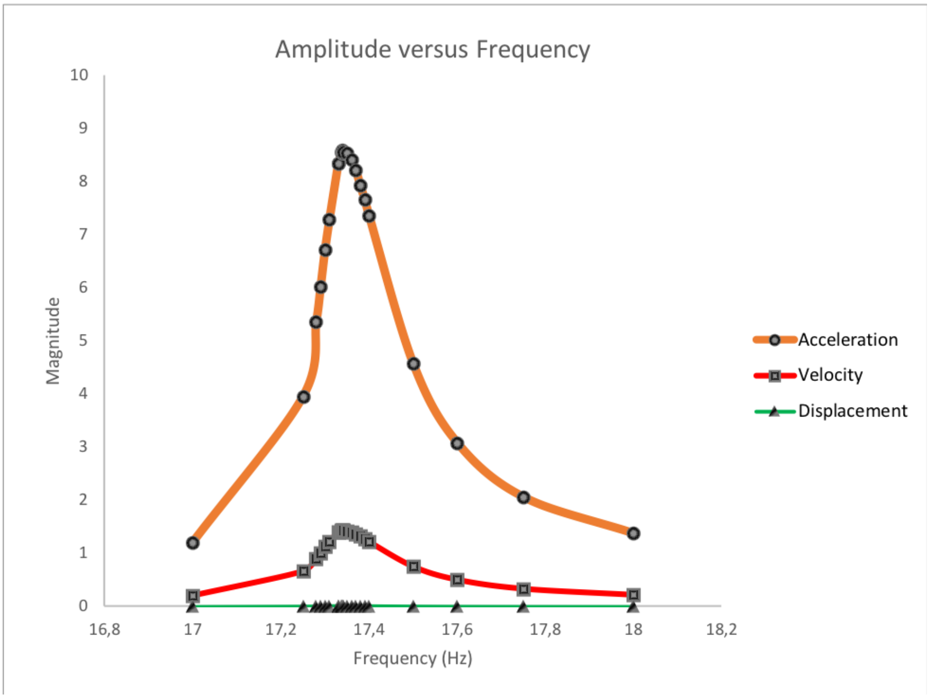

Figure 2: Comparison of the Magnitudes.

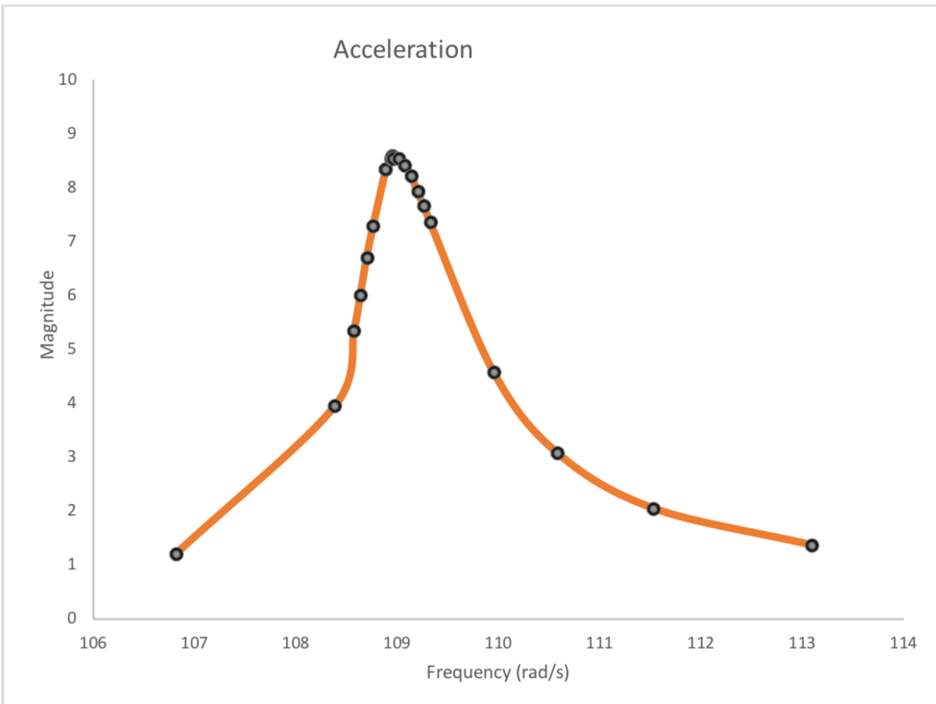

Figure 3: Acceleration Magnitude versus Frequency.

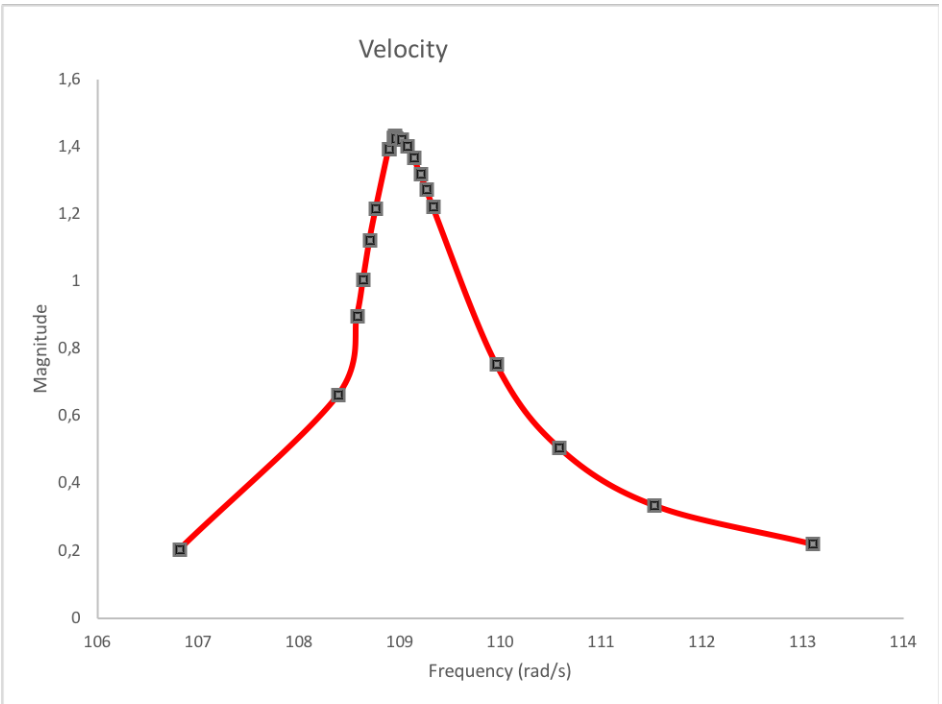

Figure 4: Velocity Magnitude versus Frequency.

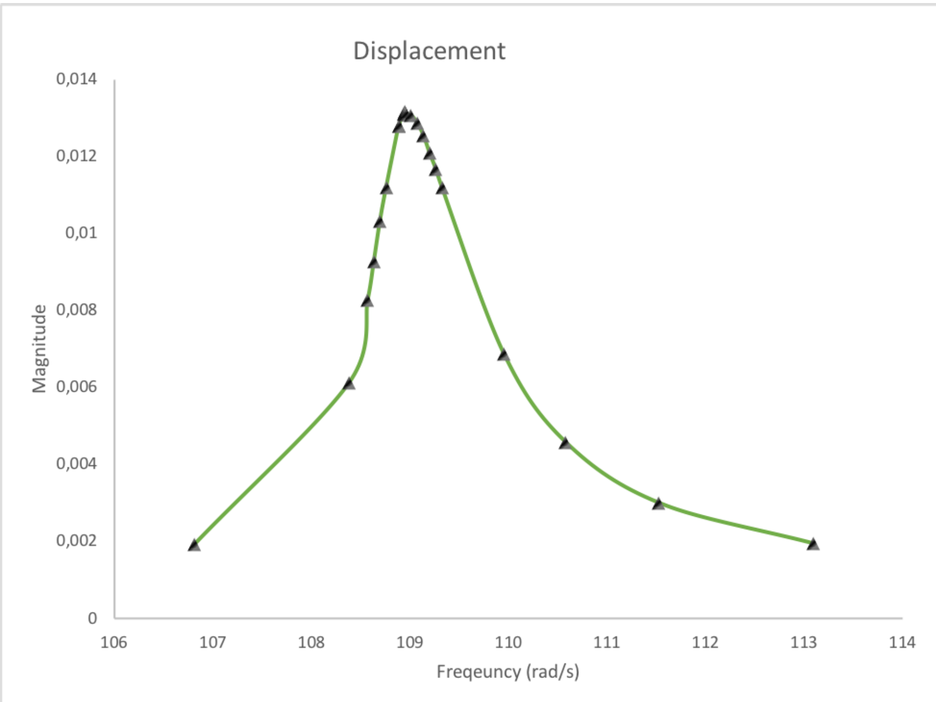

Figure 5: Displacement Magnitude versus Frequency.

The phase angles against the forcing frequency graph for Acceleration, Velocity and Displacement are plotted (see Figure 6).

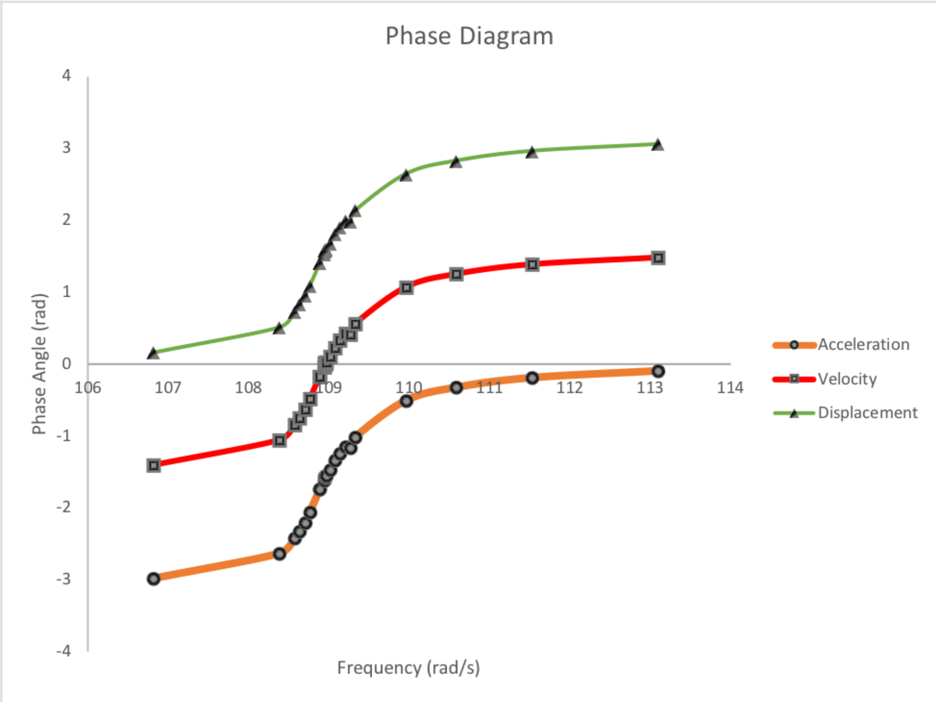

Figure 6: Comparison of the Phase Angles.

The respective Nyquist plots for Acceleration, Velocity and Displacement are represented here (see Figure 7,8 and 9).

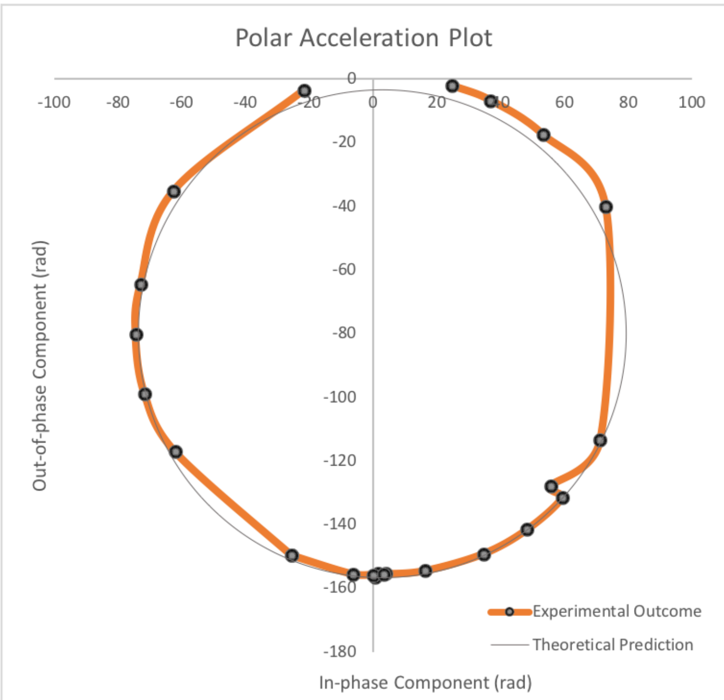

Figure 7: Nyquist Plot of Acceleration.

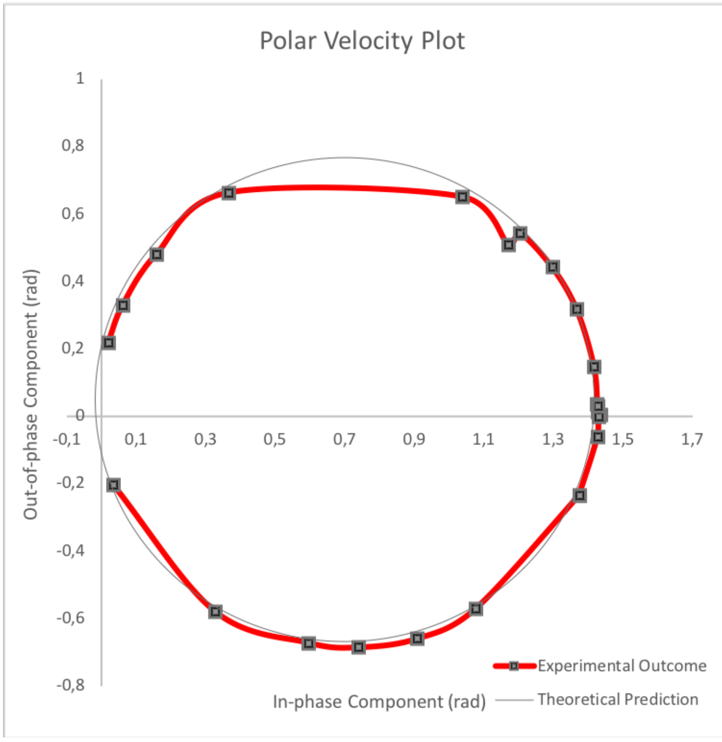

Figure 8: Nyquist Plot of Velocity.

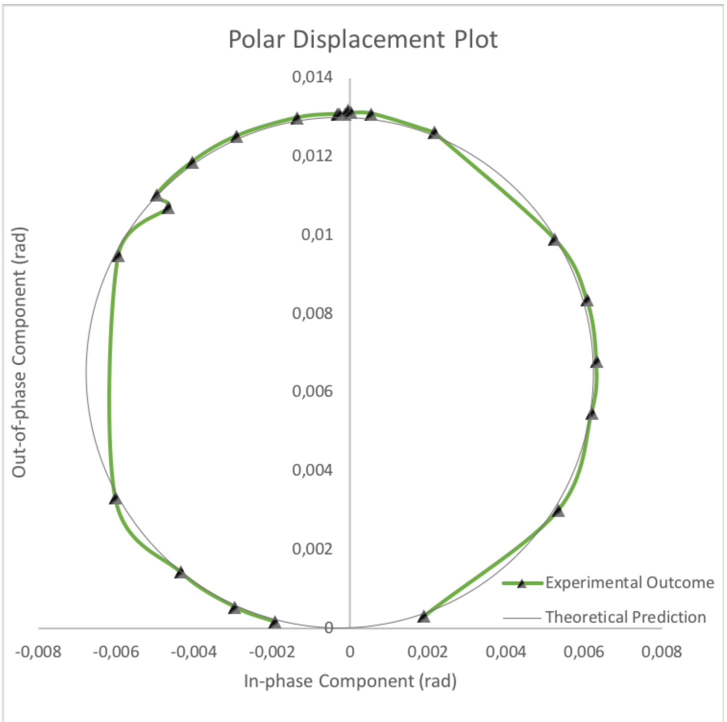

Figure 9: Nyquist Plot of Displacement.

Theory predicts that a Nyquist plot should form a circle, however, due to measurement errors and other external factors that were described in Section 3.1.1 the experimental data does not create ideal circles. The smallest error between the theoretically predicted polar plot and the experimentally obtained circle occurs in the Polar Displacement Plot (about 94.3 % quality fit). The most significant error occurs in the Polar Acceleration Plot where the quality fit is only approximately 93.7%, whereas the Polar Velocity Plot has a discrepancy of about 6.0%.

3.1.3 Calculation of Undamped Natural Frequency and Damping Ratio

The formulae to calculate undamped natural frequency and damping ratio are given below:

$$\omega_u^2 = \frac{\omega_A^2 \omega_B \tan\theta_{\dot{r}B} - \omega_B^2 \omega_A \tan\theta_{\dot{r}A}}{\omega_B \tan\theta_{\dot{r}B} - \omega_A \tan\theta_{\dot{r}A}} \tag{1}$$

where ω_u is the undamped resonant frequency, $\theta_{\dot{r}}$ is the velocity phase and ω_A and ω_B represent picked frequencies.

$$\zeta = \frac{1}{2\omega_u} * \frac{\omega_B^2 - \omega_A^2}{\omega_B \tan\theta_{\dot{r}B} - \omega_A \tan\theta_{\dot{r}A}} \tag{2}$$

where ζ is the damping ratio and other values have the same meaning as in the formula above.
From Table 1, the highest magnitude was obtained at 17.34 Hz, to find the desired natural frequency two frequencies that are as close as possible to this value have to be picked. Therefore, 17.339 Hz and 17.341 Hz are chosen as ω_A and ω_B respectively. Applying the equations (A.2) and (A.4) from the appendix A, $\theta_{\dot{r}B}$ and $\theta_{\dot{r}A}$ can be found. Hence using equation 1:

$$\omega_u^2 = \frac{17.339^2 * 17.341 \tan(0.0252) - 17.341^2 * 17.339 \tan(0.0104)}{17.341 \tan(0.0252) - 17.339 \tan(0.0104)}$$

$$\omega_u = 17.34 \text{ Hz}$$

Damping ratio ζ therefore can be determined using equation 2:

$$\zeta = \frac{1}{2 * 300.6} * \frac{17.341^2 - 17.339^2}{17.341 \tan(0.0252) - 17.339 \tan(0.0104)}$$

$$\zeta = 7.78 * 10^{-3}$$

For more detailed derivations of equations 1 and 2 see the laboratory handout (1). Comparison of Numerical and Experimental results can be seen in Table 1.

Table 1: Theoretical and Experimental Frequencies and Damping Ratios.

	Resonant Frequency (Hz)	Damping Ratio
Theory (Lumped-mass)	15.69	0.00
Theory (Point-mass)	15.65	0.00
Experiment	17.34	$7.78*10^{-3}$

3.2 Mode Shape

Comparison of theoretically obtained eigenvectors (using point-mass approximation) and the experimental ones (See Table 2).

Table 2: Numerical and Experimental Eigenvectors for each mass point.

Accelerometer Position	1	2	3	4	5	6	7	8	9
Numerical	0.051	-0.054	-0.15	-0.353	-0.639	1	0.118	0.118	1
Experimental	0.026	-0.031	-0.154	-0.324	-0.592	0.977	0.110	0.094	1
Absolute Difference	0.025	0.023	0.004	0.0289	0.047	0.023	0.008	0.024	0
Deviation %	49	43	2.7	8.2	7.3	2.3	6.8	20.3	0

A visual compilation of the deformed aircraft model (see Figure 10).

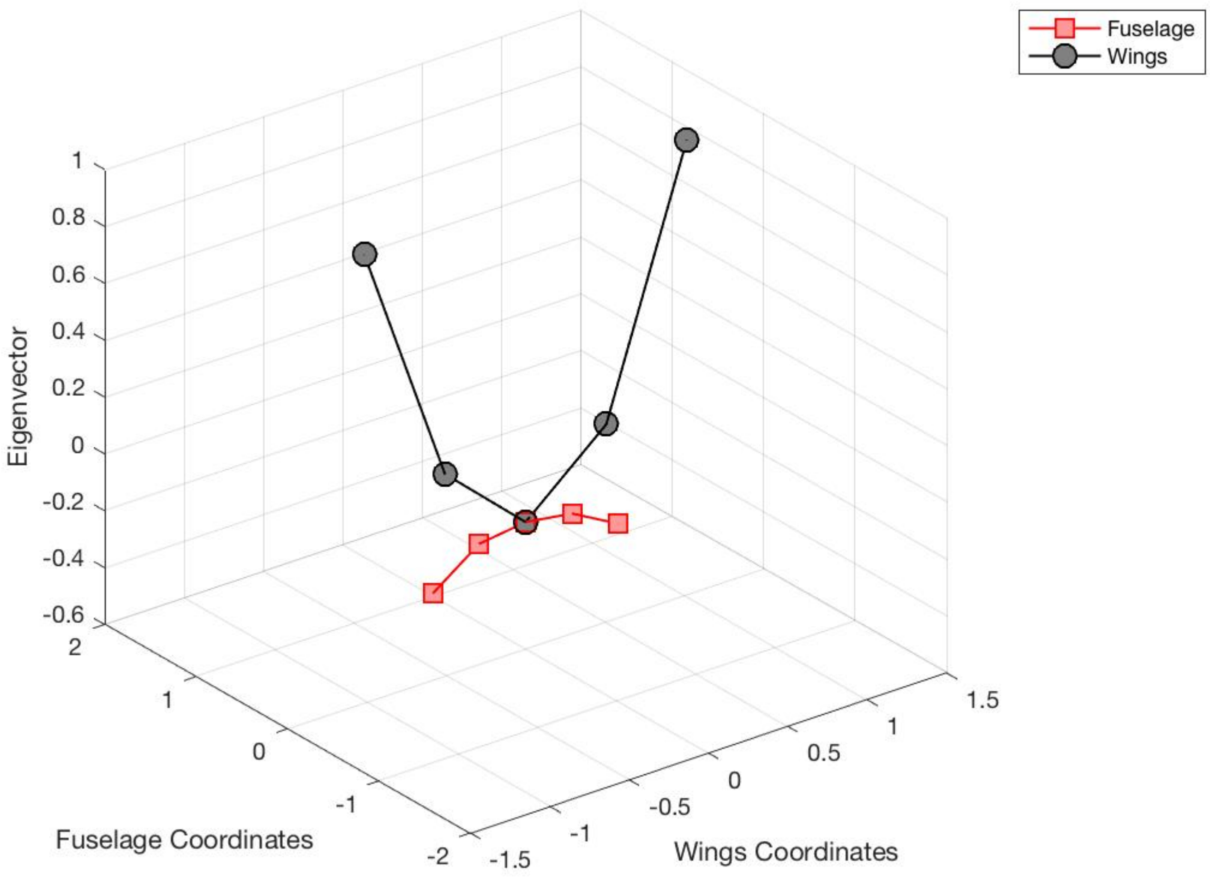

Figure 10: 3D Model for the first mode shape using Matlab.

Now, one can compare numerical point-mass eigenvectors and the deformed shape of the model.

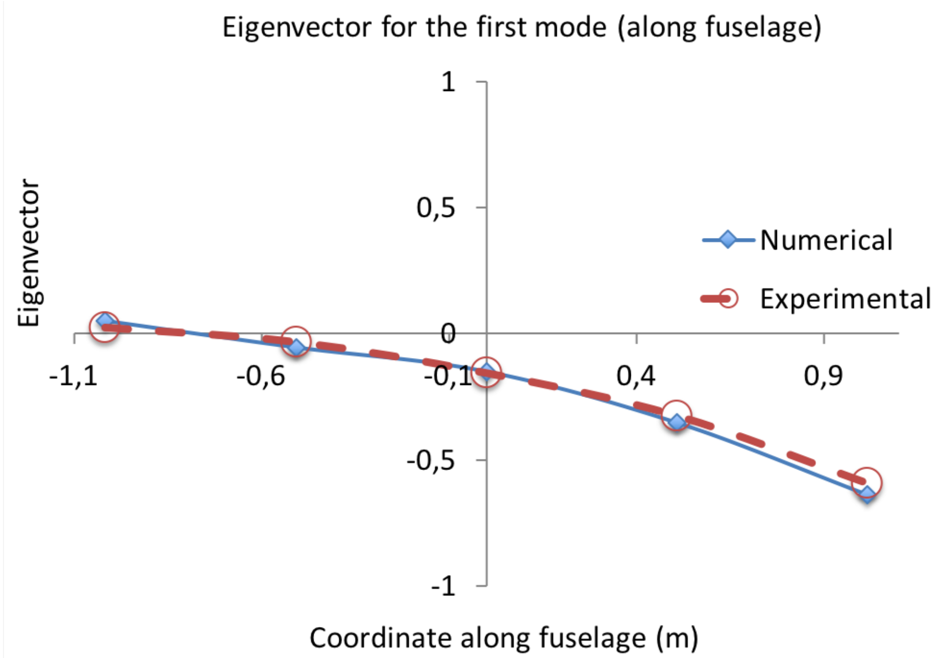

Figure 11: Comparison of Theoretical and Experimental Eigenvectors for the fuselage.

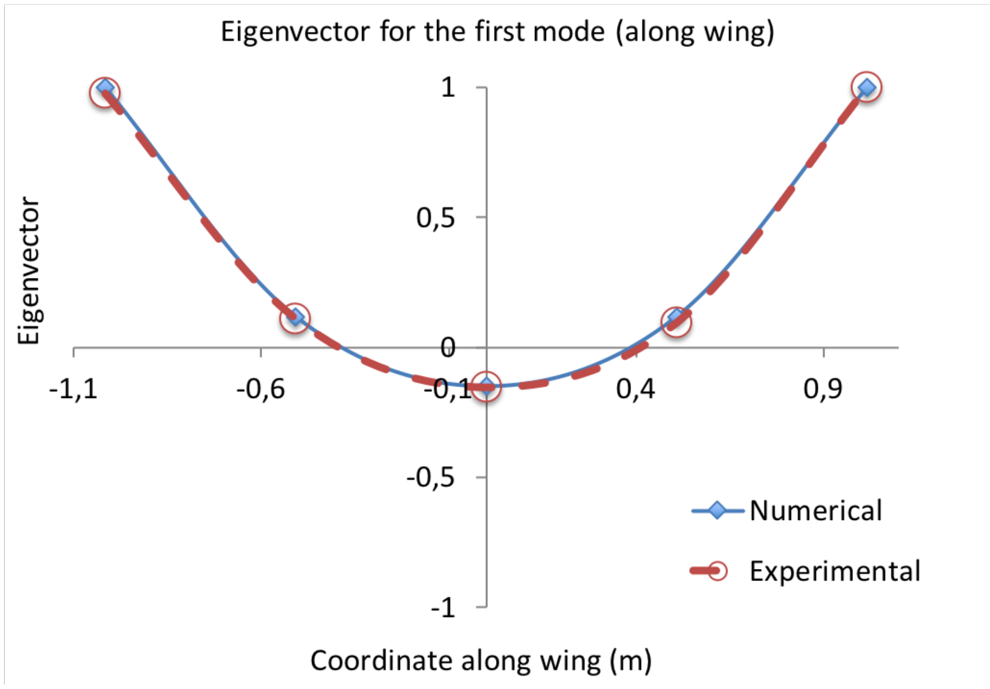

Figure 12: Comparison of Theoretical and Experimental Eigenvectors for the wings.

4 Discussion

4.1 General Discussion

In this section factors influencing both Mode Shape and Frequency Response are described. The random error factors, such as temperature and pressure fluctuations, noise from people walking and talking during the experiment affected the obtained data. The stiffness k and the damping constant c are generally non-linear; therefore the application of linear formulae is not particularly accurate (4). Also, k and c changed throughout experiment due to heating effects inside of the structure and fatigue of the metal. External oscillations of the aircraft, while the shakers were switched off, distorted the applied accelerator force. Another factor is the precision of the machine. The fluctuations in the reading values were significant and due to the time restriction of the experiment only two data points were taken for each input frequency. The linearity assumption is a convenient way to analyse the aircraft model; however, the force did not have a pure sinusoidal component.

4.2 Frequency Response

The frequency found from the Nyquist plots is 17.34 Hz according to to Table 1. This value is similiar to the observed natural frequency from Figure 4 where the magnitude is maximum at 17.35 Hz (109.01 rad/s). Therefore there is an insignificant 0.01 Hz difference. However, the difference between the theoretical (point and lumped mass) and the experimental value is large, about 1.69 Hz and 1.65 Hz, i.e. experimental is 10.8% and 10.5% respectively higher than the theoretical value.

From Figures 7 to 9 it can be seen that the average error for Nyquist Plots is only 6.0%, and since a margin of error of 10% (2) is generally considered acceptable. Therefore, the accuracy of the natural frequency obtained from those graphs has high accuracy. One can notice that there is one data point which lies outside of all three circles. This point does not follow the circular pattern and dramatically affects the quality fit of the experimental plot. Besides, one can notice that there is a lack of data points far away from the resonant frequency due to a wrong approach of the students to collect the data.

The circles were not expected to be perfect, since this would be the case for an undamped structure. From Figure 2, the peak of each curve is not sharp which means that damping was significant throughout the experiment (5). Besides, from Figure 6 it can be observed that the transition region was not steep, which indicates that the damping could not be neglected and hence was significant.

Figures 3 to 5 show the theoretically predicted trends, i.e. there is a point where the magnitude is maximum and this of course happened at the resonant frequency. The normalised maximum amplitudes for the respective parameters are (see Equations

(A.1) and (A.2)):

$$||\ddot{r}|| = 156.4V \qquad ||\dot{r}|| = 1.435V \qquad ||r|| = 0.0131V$$

4.3 Mode Shape

Different resonance modes perturbed the first mode shape, since the first mode shape can be imagined to be a fraction of the second mode shape. It can be handy to visualise the mode shapes of a simple rope with nodes and antinodes, where the first mode of the rope 'sits in' the second mode, hence disrupting it. Coupling of different modes (especially if the difference in frequencies is low) interfered the first mode shape.

Since the eigenvectors were normalised to the point-mass 9 the wing eigenvectors are the greatest, therefore the first mode involves the wings more.

The absolute percentage differences for the first two points and the point 8 are prominent according to Table 2 and are about 49% , 43% and 20% respectively.

According to Martin Williams Book (4) it is common to assume the linearity of k and c to simplify the analysis of a structure, however, in real engineering problems these coefficients are not considered to be linear.

5 Conclusions

The natural frequency of the aircraft was determined to be 17.34 Hz at the damping ratio of 0.0078. After that the undamped frequency was compared to the graphically observed frequency and the theoretical predictions, i.e. both point and lumped mass. The average discrepancy of 10.65% proves the unsuitability of the assumptions made. The mode results are somewhat ambiguous, from Figure 10 the deflected shape resembles theory, however the average deviation there is 15.5%. Nevertheless, the numerical simulation matches well with theory according to Figures 11 and 12. Hence, the numerical method can be used nowadays to predict deflected shapes of n degrees structures.

The experiment could have been improved by moving the general setup to a quieter place where the would be no external noises as well as no temperature changes. Alternatively, higher amplification factor with a higher saturated voltage device could be used. The precision could also have been enhanced by using all nine accelerometers instead of just one. To reduce a random error, the experiment needs to be repeated a few more times.

References

[1] Dr Silvestre T Pinho. *Vibrations of an Aircraft Model. Laboratory Handout.* Department of Aeronautics, Imperial College London. pages 5, 11

[2] Anne Helmenstine. *Sources of Error in Science Experiments. https://sciencenotes.org/error-in-science/, 6 November 2016.* pages 14

[3] Dr Silvestre T Pinho. *AE2-213 Structural Dynamics, 2018.* Department of Aeronautics, Imperial College London. pages

[4] Martin WIlliams. *Structural Dynamics, 2016. Section 5.2. Non-linearity in structural properties.* pages 14, 15

[5] Hans Anton Buchholdt and Shodja Edin Moossavi Nejad. *Structural Dynamics for Engineers,* 2^{nd} *Edition ,2012. Section 5.3 Vibration at resonance.* pages 14

Appendix A: Additional Formulae

$$\|\dot{r}\| = \frac{\|\ddot{r}\|}{\omega} \tag{A.1}$$

$$\theta_{\dot{r}} = \theta_{\ddot{r}} + \frac{\pi}{2} \tag{A.2}$$

Equations A.1 and A.2 represent the formulae which were used to find the Magnitudes and Phase Angles of Velocity.

$$\|r\| = \frac{\|\dot{r}\|}{\omega} \tag{A.3}$$

$$\theta_{r} = \theta_{\dot{r}} + \frac{\pi}{2} \tag{A.4}$$

Equations A.3 and A.4 represent the formulae which were used to find the Magnitudes and Phase Angles of Displacement.

$$\mathbf{M}\ddot{\mathbf{r}}(t) + \mathbf{K}\mathbf{r}(t) = 0 \tag{A.5}$$

The equation of motion for a structure with n degrees of freedom with no damping and under free vibrations.

$$(\mathbf{K} - \omega_u^2\mathbf{M})\varphi = 0 \tag{A.6}$$

The Eigenvector problem for the experiment.

Appendix B: Raw data for the determination of resonant frequency and damping ratio

Table 3: Experimental Data

Frequency (Hz)	Amplitude factor (V)	Read Magnitude (V)	Read Phase (rad)
17.000	0.055	1.206	-2.9797
17.250	0.055	3.9530	-2.6288
17.500	0.055	4.5750	-0.5024
17.750	0.055	2.0580	-0.1820
18.000	0.055	1.3720	-0.0870
17.600	0.055	3.0800	-0.3170
17.400	0.055	7.3600	-1.0098
17.330	0.055	8.3450	-1.7400
17.310	0.055	7.2880	-2.0582
17.300	0.055	6.7120	-2.1989
17.290	0.055	6.0180	-2.3193
17.280	0.055	5.3560	-2.4172
17.390	0.055	7.6660	-1.1597
17.380	0.055	7.9300	-1.1473
17.370	0.055	8.2200	-1.2415
17.360	0.055	8.4180	-1.3425
17.350	0.055	8.5400	-1.4665
17.340	0.055	8.6000	-1.5664
17.338	0.055	8.5550	-1.6122
17.339	0.055	8.5470	-1.5604
17.342	0.055	8.5500	-1.5500
17.341	0.055	8.5450	-1.5456
17.340	0.055	8.5700	-1.5716
17.330	0.055	8.3450	-1.7400

Appendix C: Pictures

The Point-mass representation of the model.

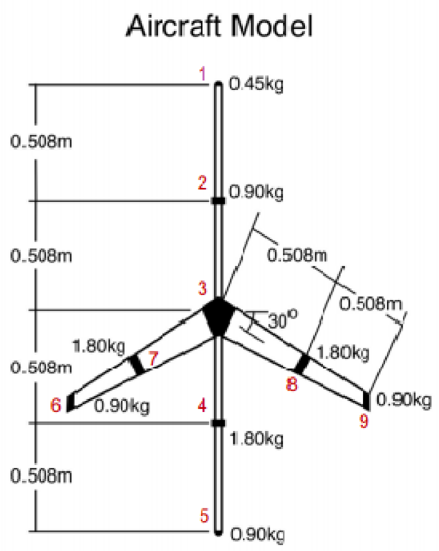

Figure 13: Point-mass representation.

The general view on the experimental setup.

Figure 14: General Setup.

The computer and the software that were used throught the experiment.

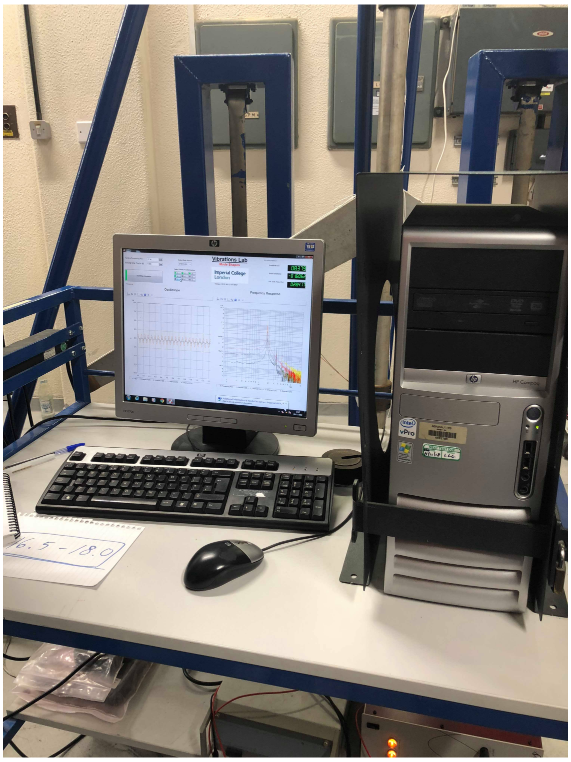

Figure 15: Computer.

The signal amplifier.

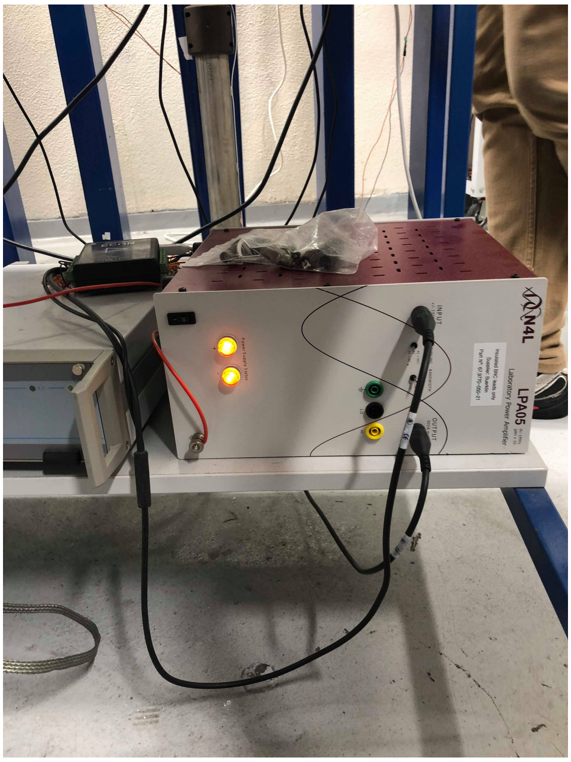

Figure 16: Amplifier.

Digital to Analogue Converter.

Figure 17: Analogue Converter.